A REVIEW OF MACHINE LEARNING METHODS TO MONITOR HEIGHT OF THE ATMOSPHERIC BOUNDARY LAYER

*Laila Abdulla** [1], *N. V. Chinnasamy* [2]

ABSTRACT

The area in air next to the Earth's place when heat, moisture, and trace elements are reduced is known as the atmospheric boundary layer (ABL). Despite being significant for a number of applications, quantitative information regarding the spatial and temporal shifts inside the width of the ABL with its sub-layers are quite lacking. The latest advances in algorithm development and ground-based ML technologies make it possible to constantly profile the whole ABL vertical level with excellent vertical as well as temporal resolution. This paper provides an overview of the several retrieval techniques generated through the identification of ABL sublayer peak from various atmospheric parameters, as well as an overview of the strengths and weaknesses of numerous sensor kinds used for ABL measuring. The effective combination of methods for monitoring the ABL's diurnal evolution is described, with a particular emphasis on areas where instrumental or methodological synergy is seen to be specifically promising. The review focusses the importance of standardizing data collection across organized SN and customized data processing in producing high-quality goods that are necessary for capturing the temporal as well as spatial complication of the lowest levels in the atmosphere where humans breathe.

Keywords: Atmospheric Boundary Layer (ABL), Unified Ceilometer Network (UCN), Planetary Boundary Layer (PBL), Machine Learning (ML)

I. INTRODUCTION

The lowest region of the atmosphere, referred to as the ABL, is where the majority of interactions between the atmosphere and the Earth's area occurs. This is important through interchange inside heat, humidity, aerosols, greenhouse gases, momentum, as well as additional atmospheric gases [1-3]. Therefore, enhanced process comprehension as well as quantitative understanding of ABL activity are necessary through the variety of process with major impacts on society, the economy, and public health [4, 5]. These applications include the evaluation of greenhouse gas emissions or air quality, the production of renewable energy, sustainable urban planning, numerical weather prediction, as well as all features of transportation, including shipping, aviation, and road safety. In recent times, radiosondes have been used mainly for ABL vertical profile sampling [6-8].

While the information gathered from these balloon ascents is essential, the whole diurnal development of the ABL activity is usually not captured by their temporal resolution, and the balloon's significant horizontal drift throughout the ascension means that observations are forced by spatial differences in the ABL dynamics, that can make interpretation difficult as well as data analysis [9]. Ground-based ML started to overcome this gap in recent decades by offering high- resolution data, first focusing on the lowest kilometer of the atmosphere [10]. Significant advancements in algorithm development and ground-based ML technology now allow automatic identification of ABL sub-layer heights through various atmospheric parameters, as well as nonstop profiling of full ABL vertical degree at tall temporal as well as vertical resolution [11]. Figure 1 shows the architecture of Atmospheric Boundary Layer.

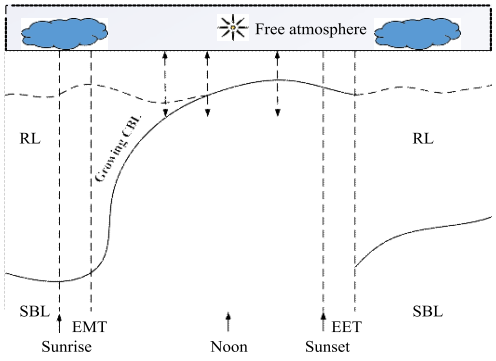

Figure 1: Architecture of ABL

Department of Computer Science[1],
laila.abd@gmail.com[1]
Department of Computer Science[2]
Karpagam Academy of Higher Education, Coimbatore, Tamil Nadu, India
* Corresponding Author

Recently, a variety of remote sensing tools have been utilized extensively to describe the ABLH, include microwave radiometers, Doppler lidars, and elastic lidars ceilometers. Ceilometers are one of these remote sensing instruments that has the benefit of being cheap and low maintenance for monitoring clouds and aerosol layers [12]. These features have made drawback of using ceilometers to measure ABLH is that it can be difficult to differentiate between SBL height (SBLH) and RL top height during steady periods. The problem arises from the basis of the ceilometer detection protocol, which based upon vertical outline of atmospheric can obstruct the identification of the highest thermal inversion within this particular case [17, 18]. Regarding these details, it is still possible to improve the ABLHretrieval process using ceilometers by employing different data processing techniques for the ceilometer's output. In the past few years, ML methods are used extensively inside the environmental skills. These machine learning algorithms have shown effective in various atmospheric fields, including the approximation of atmospheric limitations like the collapsing layer height. They are capable of considering complex interactions on atmospheric processes [19, 20]. The main objective of this review is to give an extensive review of the most recent ABL describing methods are making relevant data available. Then the remaining portion of this review paper contain: sublayers of the atmospheric boundary layer is presented in Section 2. Section 3 contains the Characterization of atmospheric gases and thermodynamic variables. Section 4 provides the retrievals of ABL height. Section 5 contains the classification of ABLH. Section 6 shows the machine learning methods that used for monitoring ABLH. Section 7 has metrics and graphs used for ABLH. Section 8 contain conclusion of the review.

II .LITERATURE REVIEW

2.1 The sublayers of the atmospheric boundary layer

The lowest layer of the troposphere is called ABL, sometimes called planetary boundary layer. It is the area of the atmosphere that the Earth's surface directly affects. The characteristics of the Earth's surface, including temperature, humidity, roughness, and vegetation cover, have a direct impact on the ABL. The height at which this influence extends upward can vary significantly, from a few hundred meters to a few kilometers.

Topography, or the shape of the land surface, wind shear, or the variation in wind speed as well as direction through height, and solar surface heating all add to the height of the ABL. Figure 2 shows the sublayers of atmospheric boundary layer.

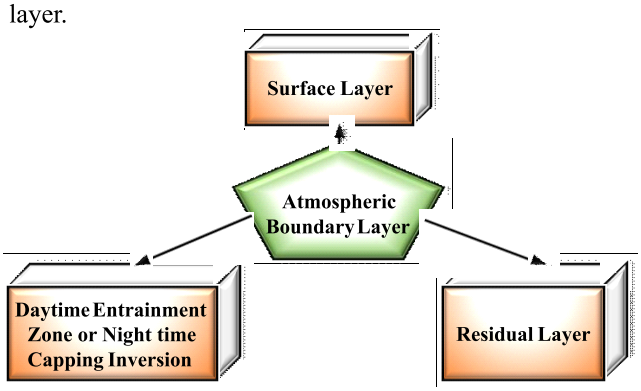

Figure 2: Block diagram of atmospheric boundary layer

The ABL is referred to the most turbulent layer of the atmosphere due to its near connection through the Ground's surface. Convection, the movement of moisture and heat through floating air parcels rising into the atmosphere, and frictional drag from the surface, resulting in mechanical mixing, are the two main causes of turbulence. During the day, when the sun heats the Earth's surface, convection is usually highest. Within the ABL, vertical motions and mixing is produced by the warmed surface air rising to the surface and becoming buoyant. Three sublayers can be identified within the ABL:

2.1.1 Surface layer

Guan et al. [21] suggested a Boundary conditions and the explicit solution of atmospheric Ekman flows' dynamic properties. Then examine the classical problem of wind in the steady-state atmospheric Ekman layer with constant eddy viscosity in this research. Using the notation of matrix cosine and matrix sine,then modify the boundary conditions as well as derive the explicit solution in a different way than the prior

work. The ABL's lowest sublayer, usually reaching no higher than 100 meters from the Earth's surface. Structures include flora, structures, and bodies of water that are directly impacted by the rough texture of the Earth's surface. The roughness factors influence the highly varying wind velocity and direction within the surface layer. For instance, compared to smooth areas like open water, wind speed will be slower and more turbulent over difficult terrain like lumber. In the surface layer, there is also a noticeable vertical gradient in both humidity and temperature. This indicates that the warmest as well as most humid air is located closest to the surface, and that temperature and humidity vary quickly with height.

2.1.2 Daytime entrainment zone or nighttime capping inversion

Khalesi et al. [22] introduced an In- depth time-series examination of temperature inversions in Tehran's urban air boundary layer between 2014 and 2018. Tehran, a city in northern Iran with a population of over 8,700,000, acts as the study area for this work (SCI 2016). With an 800-km2 surface area, Tehran has a mean elevation of 1200 m above sea level (ASL) and is geographically organized between 35°41′39°N and 51°25′17°E in the north and east, respectively. The uppermost ABL sublayer, which divides the ABL from the upper free atmosphere. When the Earth's surface gets heated by the sun throughout the day, the entrainment zone is present. In contact with the surface, the air heats and becomes buoyant additionally. ABL air and air from the free atmosphere above are mixed together as a result of the buoyant air rising through the ABL and causing turbulence. Strong vertical wind shear, or the quick change in wind direction and speed with height, is a feature of the entrainment zone, which is normally only a few hundred meters deep. On the other hand, a warm air layer known as the capping inversion develops overnight above the ABL. At night, heat from the Earth's surface reflects back into space, causing the air close to the surface to cool and forming this layer. The warmer air above becomes trapped as the colder air gets thicker and sinks. Heat and pollutants could become trapped in the ABL because the capping inversion prohibits vertical mixing.

2.1.3 Residual layer

Wang et al. [23] demonstrates that a crucial step in the atmospheric nucleation process during haze episodes is the descending mixing of tall SO2 air through the morning RL towards the area. When the haze event occurs by high concentrations of SO2 carried by prevailing winds via tall smokestacks outside of Beijing, as well as the high SO2-containing air is held within the RL later sunset. The night-time residual layer was released by vertical collapsing as well as SO2 was progressively carried into the surface level when the sun rises as well as surface heating increases. A layer of a little stagnant air that develops above the surface level at night is known as the residual layer. It is a piece of the daytime ABL that radiative cooling isolates from the surface. The violent mixing that defined the daytime ABL lessens as the sun sets as well as the Earth's surface cools. In order to prevent the colder airat the surface from rising and combining with the warmer air above, it becomes denser and more stable. The heat and pollution generated at the surface throughout the day gets trapped in this stable layer of air. After sunset, the leftover layer could remain for a few hours till the sun rises again and starts to warm the surface. Depending on the strength of the winds above and the degree of nighttime cooling, the residual layer's depth can change. When winds are severe enough, turbulence may sometimes totally dissolve the residual layer. On the other hand, in calm circumstances, the residual layer could remain all night and significantly affect air quality, especially in cities where pollutants may become trapped close to the surface.

2.2. Characterization of atmospheric gases and thermodynamic variables

Sherbo et al. [24], introduced the complex mixture of gases that makes composed the atmosphere varies in concentration according to time, place, and altitude. The two main elements that make up more than 99 percent of the atmosphere are oxygen (O_2) and nitrogen (N_2). With 78% of all gases being colorless and odorless, nitrogen is the most common. Its ability to absorb small amounts of solar light and thermal energy makes it necessary for controlling temperature and preventing major changes. At 21%, oxygen

is a necessary component of life on Earth and is constantly transformed by plants and animals through photosynthesis and respiration. Figure 3 shows the characterization of atmospheric gases.

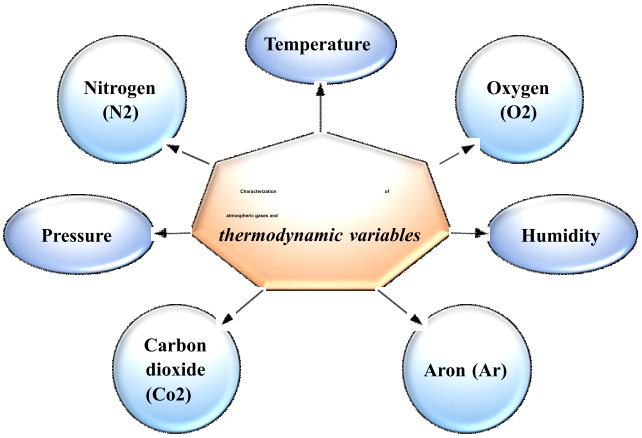

Figure 3: Characterization of atmospheric gases

Here, Lee et al. [25] suggested a hydrogen bonding and Lewis acid-base combinations influence the permeability of CO2 and CO2/N2 selectivity. Although they are present in significantly smaller dimensions, argon (Ar), carbon dioxide (CO2), and water vapor (H2O) are other significant atmospheric gases. The third most common gas, argon (Ar), has an abundance of 0.93% and is inert, or it does not react effectively with other elements. Around 0.04% of Earth's surface is made up of carbon dioxide (CO2), a greenhouse gas that traps heat radiation and raises the planet's temperature. But in recent decades, human activities including burning fossil fuels have raised CO2 concentrations significantly raising fears about climate change. Depending on temperature and location, water vapor (H2O) can be found in trace levels or in significant amounts in the atmosphere. It is one of the most abundant changeable gasses. It is necessary for precipitation, cloud formation, and weather patterns.

Wen et al. [26] introduced to evaluates quantitatively the spatial as well as temporal changes in unpackaged and computed dry N statement data in China between Nineteeneighty and twenty eighteen. According to a long-term dataset covering 1980 to 2018, large N deposition highest point about 2000 as well as has decreased by 45% through the years 2016 to 2018. Recent observations from 2011 to 2018 show a decrease in dry N as well as bulk deposition. This odorless along with colorless gas makes up approximately four-fifths of the atmosphere's total volume, making it the most prevalent component. Nitrogen gas (N2) has a strong triple bond among its two nitrogen atoms, which makes it relatively unreactive yet being essential to life on Earth. Because nitrogen is non-reactive, it can act as a buffer to reduce extremes in temperature that might otherwise happen on Earth. Furthermore, nitrogen gas is essential for biological functions. Nitrogen becomes an essential plant nutrient when it is transformed by certain soil microorganisms into ammonia (NH_3). The nitrogen cycle is ultimately completed when nitrogen is released again into the atmosphere during the process of decomposition.

Morelli et al. [27] aim to highlight the significance of O2 passive transport through lipids in many, if not all, aerobic species. In particular situations, this transport is likely to be the primary method. Lipids are essential for gas exchange in plants, which involves the absorption of CO2 and release of O2. The majority of multicellular organisms, including mammals, breathe air to get oxygen. Through their gills, fish along with other aquatic life absorb dissolved oxygen from the water. Through a process called photosynthesis, which requires carbon dioxide, water, and sunshine to make glucose (sugar) and oxygen, plants are able to produce oxygen. For the atmosphere to remain oxygen-rich and to support life on Earth, plants must produce a net amount of oxygen.

Graven et al. [28] suggested how human activity and its effect on the natural carbon cycle have altered the carbon isotopic composition of atmospheric CO2 since the Industrial Revolution, and then offer updated predictions of potential future changes for different scenarios. One naturally occurring gas that is essential to the functioning of Earth's atmosphere is carbon dioxide (CO_2). As a greenhouse gas, it absorbs heat emitted by the sun and raises the planet's surface temperature. Because it keeps the

temperature range inside a habitable range, the greenhouse effect is crucial to life as recognize it on Earth. The main cause of the global climate change, which is having a number of disturbing consequences such as melting glaciers and polar ice caps, rising sea levels, and higher global temperatures, is this increase in CO2 concentration. The vast majority of researchers agree that immediate action is required to cut greenhouse gas emissions and lessen the effects of climate change.

Xie et al. [29] examined that spatiotemporal (intra-annual, diurnal, as well as inter-annual) changes within land surface temperature (LSWT) of China's shares between 2001 and 2016 utilizing MODIS-LST data. Using multivariate regression analysis, this study also conducted a quantitative investigation between the lake morphometry, topography, and surface temperature as well as the diurnal temperature differences. For some majority of ponds, correlation analysis between the trends in air temperature and LSWT showed a positive relationship between the two variables over both the day and night. The position at which sunlight strikes the Earth's surface causes temperatures to be generally warmer at the equator than at the poles. Variations in the seasons also matter; summer temperatures are greater due to longer days and more exposure to the sun.

Phillips et al. [30] describes the air-sea interactions, climate variability, and circulation patterns in the Indian Ocean, bringing together new knowledge about the ocean-atmosphere system since the last thorough review. A concerted global emphasis on the Indian Ocean has spurred the use of new technology to provide observations and simulations of Indian Ocean dynamics with more detail. Finally learning about the importance of small-scale processes in determining large-scale gradients and circulation, as well as the relationship between boundary currents and the interior, physical and biogeochemical processes, and the surface and deep ocean. Table 1 shows the comparison of atmospheric gases and thermodynamic variables.

Table 1: Comparison of existing studies

Authors	Contribution	Advantages	Limitations
[25]	Selectivity for carbon dioxide and nitrogen utilizing poly membrane molecular dynamics investigation.	Used to improve membrane design.	It has high computational complexity
[26]	Variations in China's nitrogen deposition between 1980 and 2018	It highlights the source variations	It not considered the affecting deposition
[27]	The Importance of Lipids in Biological Organisms' Absorption and Release of Oxygen	Increase the knowledge about a variety of organisms	Minimal experimental data
[28]	Changes in atmospheric CO2's carbon isotope composition during the industrial period and in the future	Isotope ratios help in verifying the carbon cycle predictions of climate models.	The carbon cycle's complexity
[29]	MoDIS temperature data is utilized to analyze the surface temperature change of lakes in China.	Extended -Term Data Availability	Assesses Land Surface Temperature, Not Actual Water Temperature

Authors	Contribution	Advantages	Limitations
[30]	Understanding of the circulation, variability, air-sea exchange, and effects on bio-geochemistry of the Indian Ocean has advanced.	Improved management of maritime resources	Model intricacy

2.4 ABL height retrievals

The lowest part of the troposphere, or the layer of the atmosphere nearest to the Earth's surface, is known as the Atmospheric Boundary Layer (ABL), commonly referred to as the Planetary Boundary Layer (PBL). The temperature, moisture content, and roughness of the Earth's surface all have a direct impact on the ABL. In contrast with the layers above, this effect generates a layer with unique qualities. Because of the turbulent movements carried on by the ground's solar heating, the ABL is typically well-mixed. The ABL's height (ABLH) changes in different parts of the world and during the day and night. Figure 4 shows the block diagram of ABLH.

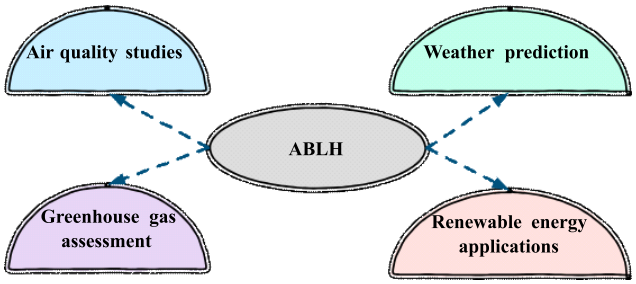

Figure 4: Block diagram of ABLH

Marley and Hannah Gwen [31] suggested An Experimental Examination through the Air Pollution as well as Atmospheric Boundary Layer Elements That Affect the Development of Winter Brown Haze in a Complex Coastal Urban Area. In an urban location with complex coastal topography, this thesis offers a better knowledge of the structure and dynamics of the ABL and their impact on the horizontal as well as vertical mixing and dispersion of winter air pollution and brown haze. This was accomplished by the use of case studies from Auckland, New Zealand, that were based on long-term, continuous synoptic scale (Kidson weather types) and local datasets. Scientists may predict how contaminants will spread through the ABL and affect the quality of the air that breathe at the surface by knowing its height. Pollutant movement within the ABL is additionally affected by wind direction and speed. As a result, precise ABLH retrievals are essential for releasing air quality advisories and putting into practice effective pollution control plans.

Focusing on both experimental and modelling viewpoints, Giovannini et al. [32] introduced current findings and advancements in this field. In order to better comprehend and demonstrate the atmospheric mechanisms governing the fate of pollutants over hills, itdraws attention to some unanswered questions and challenges. For instance, in order to avoid hazardous pollutants building up close to the ground, power plants could be requested to lower their emissions during times of low ABLH. On the other hand, pollutants may become more widely distributed during times of high ABLH, which will decrease their effect on surface air quality.

Che et al. [33] suggested that Tibetan Plateau is a region which is very sensitive to changes in the global climate. Its unique along with intricate land surface as well as boundary layer procedures have a significant thermal and dynamic impact on the overall circulation and climate. This research for the first time reveals significant east–west changes within ABL height, diurnal amplitude, and occurrence frequency throughout the TP portion through summer, thanks to fresh sounding measurements in the WTP. An important variable in numerical weather prediction approaches is ABLH. These models are complicated to computer programs that replicate the behavior of the atmosphere. ABLH affects

wind shear, turbulence, and atmospheric stability of all which have a big impact on weather patterns. For instance, important convection and the formation of thunderstorms might result from a high ABLH. Lelandais et al. [34] suggested the atmospheric position information gathered through OHP, a rural south-eastern France station on the ICOS-France atmospheric greenhouse vapors network. The OHP 100-meter height tower continuously gathered meteorological data as well as CH4, CO2, and CO at 50 m, 10 m, as well as 100 m (AGL). The measurements along with calibration procedure correspond to the worldwide WMO-GAW scale and ICOS requirements. The ABLH affects how greenhouse gases move between the atmosphere and the surface. At the Earth's surface, greenhouse gases are released by using fossil fuels, agriculture, and natural processes, among other sources. These gases include carbon dioxide, methane, and nitrous oxide. Then, when these gasses rise through the atmosphere, they finally reach greater elevations. On the other hand, a deeper ABLH makes it easier for greenhouse gases to mix and breathe, which promotes their transportation to higher elevations.

Sommerfeld and Markus [35] suggested a wind-related light detection and ranging (LiDAR) data at a potential northern German location for an onshore AWES deployment. In addition to these observations, then produce and examine mesoscale weather research and forecasting (WRF) models that operate both onshore and offshore. Wind shear, or the change in wind speed with height, acts as what allows wind turbines to harvest energy from traveling air. Because of the Earth's surface's frictional effect, wind shear typically occurs higher in the ABL. The vertical extent of the wind shear zone must be calculated in order to forecast the power generation of wind turbines, and this could be achieved with the use of the ABLH. For example, a low ABLH may indicate a weak wind shear zone, which could reduce the energy-extracting efficiency of the wind turbine. Table 2 shows the comparison of ABLH retrieval.

Table 2: Comparison of ABLH retrieval

Authors	Contribution	Advantages	Limitations
[31]	An Empirical Examination of the Atmospheric Boundary Layer and Air Pollution Elements That Influence the Development of Winter Brown Haze in a Complex Coastal Urban Area	Predictive Capabilities	Atmospheric Process Complexity
[32]	Complex Terrain Atmospheric Pollutant Dispersion: Difficulties and Needs for Enhancing Air Quality Measurements and Modeling	CTAPD models can evaluate how new developments will impact air quality.	Obtaining superior quality data in complicated terrain is costly and challenging.
[33]	Features of the Tibetan Highland's summers ABLH and contributing variables	Enhanced forecasting of the weather	There are data limitations, particularly in rural areas.
[34]	5 years of continuous measurements of atmospheric CO, CH4, and CO2 and monitoring network of ICOS–France.	High quality control is carried out by ICOS-France.	Time Restriction

Authors	Contribution	Advantages	Limitations
[35]	Realistic wind profiles are necessary for the optimal functioning of airborne wind energy setups.	Enhanced System Performance	Complexity of Computation

2.5. Classification of ABLH

Different grounded remote-sensing researchers offer various changing and capabilities atmospheric factors alter algorithm uncertainties, several sub-layer height retrieval approaches depend differently during the ABL's diurnal evolution was suggested by Han et al. [36]. The most significant advantages and disadvantages of the approaches for monitoring the boundary layer's height at night or in stable circumstances, morning growth, peak CBL development, along with evening decay are discussed in the section. Capabilities that are important to the characterization of the cloud- topped ABL and the entrainment zone are also included. Figure 5 shows the block diagram of Monitoring ABL heights.

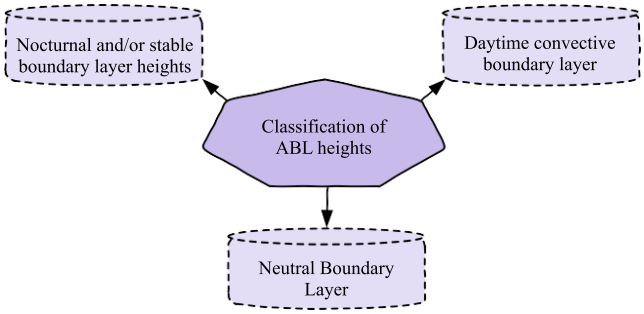

Figure 5: Block diagram of Monitoring ABL heights

A few complementary applications that are now in use are mentioned to show possible future paths for ground-based RS implementation. When explanations from various profilers were available at the same time, Wu et al. [37] analyses indicate that analyzing the results from various methods in a synergistic way may improve the explanation of the ABL, such as the identification of sub-layer statures as well as the explanation of the procedures influencing the ABL's growth. In addition, merging data from many sensor systems yields significant findings for quantifying and evaluating layer detection uncertainty which may be used to designate quality markers for the identified layer heights.

It should be highlighted that there are still few studies that Bedoya-Velásquez et al. [38] clearly compare ABL height retrievals depending on various atmospheric parameters, particularly ones that cover long time periods. Measurement setup including MWR calibration, aerosol lidar optical overlap, DWL focal setting and scan strategy, among others has an impact on layer height uncertainty. Data processing, and quality control have to be thoroughly assessed when comparing the outcomes of various techniques.

2.5.1 Heights of the nocturnal and/or stable boundary layers

The MBLH becomes rather shallow at night, and steady conditions are more frequent. A little measurement level as well as good vertical determination of the profile information is advantageous for recognizingof shallow groups was introduced by Zhang et al. [39]. Dimension uncertainties within the lowermost portion of the outline could make it difficult to determine very low layer heights for radiosondes launched using autonomous systems. The near range abilities are essential for ground-based RS instruments. Only when layer peaks reach an instrument's potential blind zone and is clear by uncertainties connected to the sensor can they be identified. Because high-power research lidars frequently fail to capture data in the lowest few hundred meters, ALCs may be more effective for detecting shallow layers when utilizing aerosol- based techniques. Figure 6 shows the stable boundary layer.

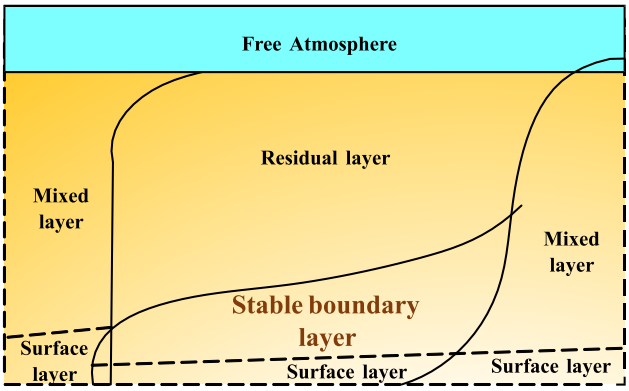

Figure 6: Architecture of Stable boundary layer

There are reported consistent differences within nocturnal MBLH among outcomes obtained from different methodologies. Garnés-Morales et al. [40] suggested that variations were found in separate groups depend on the different or same atmospheric variables through the similar order of dimensions. The identified layer elevations could differ methodically beyond thermodynamic approaches because turbulence within the SBL was typically not even. While it has been found that during stormy winters in rural Germany, turbulence-depend nighttime MBLH surpasses aerosol-depend layer peaks by an average of roughly 300 meters, average night-time MBLH variations among turbulence as well as aerosol-based approaches in UK,

London, are primarily order their daily variability. To determine how ABL atmospheric stability as well as dynamics affect the comparative agreement of the different techniques through nighttime layer height measurement, more research is required.

The best way for better characterize the nocturnal boundary layer is to employ instrument synergy. Wu et al. [41] have presented a complementary strategy to characterize the RL has no surface connected area where turbulence action is either absent and intermittent. This is achieved by utilizing a grouping of weakened backscatter as well as turbulence characteristics resulting from DWL shapes. Several studies show that, given their particular gifts in recognizing RLH and SBLH features, synergy examination of aerosol lidar as well as MWR information was particularly hopeful for nighttime layer calculation.

2.5.2 Convective boundary layer during the day

The majority of MBLH detection techniques work more effectively in the day, particularly when the CBLH and ABLH coincide. By using suitable data processing and a good ratio of signal to noise, CBLH through all approaches of retrieval can decide within a rare hundred meters or fewer, Layer et al. [42]. Layer attribution can be a general source of confusion because the CBL might not attain its complete amount if radiosonde rises at midday are related with ground-based RS profile information's. The fully developed CBL is frequently invisible to sensors with low SNR in the afternoon, in particular situations with deep boundary layer expansion, low aerosol load,along with important outside noise.

Liu et al. [43] bring attention to the possibility that a thick EZ, which most likely occurs throughout deep afternoon convection, could lead to a weaker boundary at the ABLH, raising the degree of uncertainty in layer detection across all techniques. Large shear films above the ABL present a test to turbulence-depend algorithms, but raised aerosol layers increase the risk of incorrect layer acknowledgement for aerosol-depend approaches. The air temperature profile may be further altered by layers containing advected aerosol that are different from local emissions, which could lead to mistakes in the applied thermodynamic retrieval. Thus, it has been discovered that comparison statistics are influenced by synoptic circulation persuaded flow designs which are affecting cloud circumstances of separating layers.

In clear sky conditions, the daytime highest of the layer estimations calculated using wind- or turbulence -, temperature -, as well as aerosol-depend approaches are most common, Osibanjo et al. [44]. Some works determine that CBLH using aerosol-depend approaches summits up to 2 hours other than layer statures determined through turbulence or temperature profiles, which is consistent through the late morning development on aerosol layers. The highest daytime CBLH using aerosol-depend retrievals as well as both thermodynamic or turbulence approaches have not yet been found to demonstrate a clear relationship, with

reports of biases being positive, negative, or neutral. Comparing the temperature-based conclusions from MWR profiles with the turbulence- derived CBLH DWL information revealed positive, negative, along with insignificant differences. In order to account for the presence of elevated aerosol layers, cloud dynamics, thermals overshooting the inversion at the top of the ABL, which induce vast variations in time or moisture transport and atmospheric stability, that can move CBLH growing rates, and other factors.

2.5.3 Neutral Boundary layer

Mei et al. [45] suggested that the atmosphere is vertical gradient of temperatures is almost zero is known as the neutral boundary layer. This indicates that within this layer, the air temperature stays mostly constant as one rises to higher. Like other types of boundary layers, buoyancy forces are not able to affect the air movement because there is not a considerable temperature gradient. Temperature variations lead to variations in air density, which consequently produce buoyancy forces. Cooler air is thicker and sinks, whereas warmer air is lighter and tends to rise. The buoyancy forces in a neutral boundary layer are unimportant due to the lack of temperature change, and mechanical forces dominate when assessing wind speed and direction. Figure 7 shows the architecture of Neutral boundary layer.

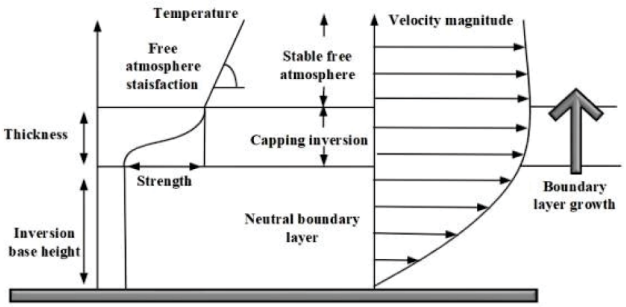

Figure 7: Architecture of Neutral boundary layer

Kakkanattu et al. [46] suggested for neutral ABLs to differentiate between flows that are truly neutral and emerge in a fluid that is neutrally stratified, and flows that are conventionally neutral and emerge against stable stratification. The totally common ABL was an idealized scenario that "doesn't appear to be within the atmosphere and uncommon that it hasn't been healthy detected," according to meteorological data spanning nearly a century. The current study will focus on the typically neutral atmospheric boundary layer (CNBL). Among the unbiassed boundary layer with the steady free air above, there is frequently a very stable, thin layer. The thickness, inversion strength, and transposal base height all affect the characteristics of this so-called covering inversion. Huge negative buoyancy services within the capping inversion slow down turbulent gusts as they try to enter the permitted atmosphere. This prevents the boundary coating becoming much deeper and slows down the turbulent entrainment procedure at the topmost within the boundary layer.

A neutral boundary layer's wind speed usually rises with height due to frictional drag on the planet's surface was suggested by Cannaby et al. [47]. The Ekman spiral, which shows a progressive veering of the wind direction with increasing altitude, describes this wind profile. The wind's deflection as it travels across the surface of the Earth, the Ekman spiral forms. This deflection acts to the left in the Southern Hemisphere and to the right in the Northern Hemisphere, is called the Coriolis effect. This means that instead of blowing straight from high pressure to low pressure, the wind close to the surface is not flowing in the same path as the pressure gradient force. As a result of the decreasing impact of surface friction, the wind is deflected at an angle, and this angle of deflection increases with height. The Ekman spiral contributes within the neutral boundary layer, winds are more likely to be stronger and more in line with the pressure gradient force as they ascend. Table 3 shows comparison of classification of ABL heights.

Table 3: Comparison of classification of ABLH

Authors	Contribution	Advantages	Limitations
[36]	For Determining the Height of the Atmospheric Boundary Layer using Polarization Lidar	It contains increased Temporal Resolution	It contains some possibility of errors
[37]	Plastic mulch film residue influences soil microorgan ISMS and their metabolic processes	Mulch film increases the activity of beneficial bacteria.	Residual plastic cannot prevent oxygen from circulating.
[38]	Situ Instruments and Short-Range Lidar to Find the Atmospheric Boundary Layer Lidar Ratio	It has high accuracy	Time consuming
[39]	Using reanalysis and AMDAR data, the diurnal climatology of the planetary boundary layer height is calculated.	Greater temporal and spatial resolution	Limited vertical resolution
[40]	Utilizing COSMIC-2 Satellite Data for Four Years of ABLH Retrievals	Elevated-Resolution data	Insufficient Spatial Resolution
[41]	During LISTOS 2019, ozone pollution episodes with PBL height variation in NYC's urban and coastal areas	Enhanced com-prehension of ozone production	Models are not accurately reflecting the complexity of pollution.
[42]	The Marine Atmospheric Boundary Layer Structure Using a Ceilometer Over the Kuroshio Current	Compared to radiosondes, ceilometers are less expensive to operate.	Only cloud base height is measured by ceilometers
[43]	When a significant haze pollution event is developing, the vertical distribution of PM2.5 is linked through the ABL	Enhanced predictions of air quality	Restricted access to data.
[44]	Anatomy of Mexico City's catastrophic ozone pollution event in March 2016	Creation of fresh modelling and monitoring methods	Limited accessing data.
[45]	Critical evaluation of the urban buoyancy-driven air flow and modelling technique	Improved Climate Simulation Accuracy	Limited Data for High Buoyancy

Authors	Contribution	Advantages	Limitations
[46]	Thermo-dynamic structure of the atmospheric boundary layer with varying sky conditions in different seasons over an Indian coastal station	Increased forecasting of the weather	Complexity of weather events
[47]	The influence of topography and Offers observational evidence rotation on the basin- scale flow in homogeneous conditions at Lough Corrib, Ireland	Offers observational evidence	Prohibited applicability

2.6 Machine learning methods for monitoring Atmospheric Boundary Layer height

Utilizing past sensor data like temperature, pressure, humidity, flow rate, and auditory signals, that could train a model to spot deviations that could point to leaks. The model has the ability to continuously scan for these abnormalities, identifying possible issues which require additional research. For instance, a sudden decrease in water pressure can be a sign of a burst pipe, whereas a rise in humidity along with a fall in temperature might be a sign of a leak in a hidden place behind a wall. Some of the machine learnings like SVM, RF, Gradient Boosted Regression Trees, KNN, DT and NB. Figure 8 indicates the comparison of ML techniques used for monitoring ABLH.

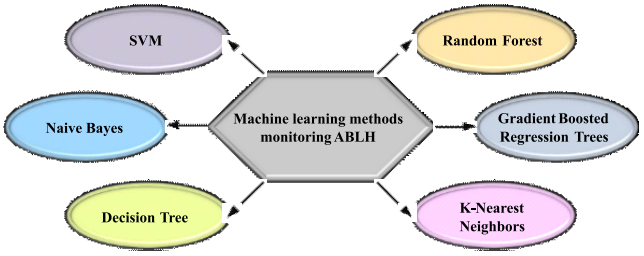

Figure 8: Block diagram of ML techniques used for ABLH monitoring

Ye et al. [48] suggested a machine learning-based approach for extracting the PBLH from ground-depend infrared hyperspectral sparkle data. Using this method, the PBLHs obtained through the radiosonde were accepted as the positive values, and the stations which are complex to humidity as well as temperature profiles were chosen as the feature paths. The data set is trained and tested using the support vector machine (SVM), which optimizes the parameters throughout the way. The data set gathered from 2012 to 2015 at SGPARM method is examined. SVMs are a useful method for tracking ABL height since they have a number of advantages. They exhibit great accuracy in real-world scenarios even in the presence of varying meteorological conditions due to their capacity to understand complex patterns from data.

Here, a random forest (RF) technique is suggested by, Li et al. [49] to determine the PBLH in complex atmospheric conditions by considering the vertical distribution of particles. An RF model input consists of the stature of the 3 minimum limited peaks oon the range correction signal (RCS) shape as well as 7 additional variables from January 2017 to December 2021, including solar radiation, relative humidity (RH), aerosol layer number, as well as other meteorological characteristics. According to the sensitivity analysis, as aerosol optical depth (AOD) increases, the relative error of the RF-estimated PBLH (PBLHRF) reduces and is less than that of the GM- estimated PBLH (PBLHGM). In addition, RF performs well under a variety of atmospheric circumstances. However, decision trees are generally poor

learners, a random forest can produce projections that are more reliable and accurate than those of any one tree by averaging the predictions of several trees. By reducing the model's variance, this method helps the model generalize better to new data and is less likely to overfit the set used for training.

However, the algorithm for machine learning recognized as Gradient Boosting Regression Tree (GBRT), de Arruda Moreira et al. [50] introduced a novel methodology has been presented for calculating the ABLH and detect the SBLH within stable conditions. Calculations of the ABLH obtained through smearing the gradient technique to a ceilometer signal as well as several surface climatological data are used by this approach as features (independent variables). The MRE among the microwave radiometer and the ABLH computed using the new method exhibit a daily pattern, with the lowest values occurring during the day and the largest values occurring at night (stable conditions). Based on current atmospheric parameter observations, the GBRT model is able to predict ABLH. This makes it possible to constantly monitor the height of the boundary layer.

Liubčuk et al. [51] first examines the basic grid component as well as how its harmonics are filtered using an IIR shelving filter. Second, inside an important section, PQ events are classified through the range of short circuit within the 3-dimensional power space and by the principal cause on the voltage– duration plane using both SVM and KNN. Thirdly, a new technique based on Clarke transformation is created to translate the resultsfrom three-dimensional space to two- dimensional space, as it appeared to interpret the outcomes in three-dimensional phases. The technique operates extremely well by preventing the loss of crucial data.

A basic foundation for calculating ABL height using typical environmental observations is provided by this decision tree, Kotthaus et al. [52]. ABL height can be a complicated meteorological quantity that is influenced by a number of variables, which is something to consider. More accurate measurements require complex techniques and specialized equipment, but this tree provides a good starting point. These include devices which provide accurate vertical profiles of temperature, wind, humidity, and aerosols: radiosondes, lidars, sodars, and ceilometers. These readings can then be analysed by sophisticated algorithms to more precisely identify the ABL top. Using development and decomposition criteria in a dynamic decision tree, layers in CABAM are traced throughout the day using sites with significant negative gradients.

While Naive Bayes provides an excellent foundation for ABL height monitoring, Jafari et al. [53] suggested to recognize its limits in order to attain the highest level of accuracy. Through statistical analysis and Naive Bayes classifiers, this study seeks that include features within IE signals which could use for efficient classification as well as analysis for bond deck evaluation. The Advanced Sensing Technology FAST NDE laboratory (FHWA) constructed eight slabs from which IE data was collected and stored in the dataset. The IE data were statistically categorized utilizing a set of temporal domain statistical features, normalized peak values, and pre-processed signal length. Naive Bayes classifiers were then used to identify the defect area. Finally, a frequency approach was used to compare the statistical categorization result. Table 4 shows the comparison of machine learning methods.

Utilizing long short-term memory networks, the temporal atmospheric boundary layer height is predicted by, Kumar et al. [54]. In order to identify ABL height on a temporal, seasonal, and annual basis, this work offers an LSTM (Long Short-Term Memory) approach that utilizes deep learning-based methods. It also identifies the underlying dynamics that determine the ABL height pattern. The SOnic Detection and Ranging (SODAR) system's measurements along with the model's outcome have been compared. The LSTM method is employed for predicting and calculating how the model affects their performance. By using the LSTM neural network, the ABL height is predicted

using both the model and observed ABL height data. This work shows that when the total amount of neurons is 32 and the epoch is 500, the best results could be achieved. Additionally, an estimation of the suggested model's performance has been made for the seasonal and annual prediction of ABL height. The findings show that for seasonal prediction, RMSE values are lowest (7.49% as well as 5.59%) during the post monsoon, highest value of (10.29% and 5.86%) for yearly prediction.

Sleeman et al. [55] suggested a technique to depth ML for lidar-based boundarylayer height detection. The impact of utilizing ground-based Ceilometer observation devices in conjunction with a ML derived PBLH (ML- PBLH) is addressed in this research. This existing study is to utilize DNN for image segmentation and denoising in ML approaches to detect PBLH in the Ceilometer backscatter signals obtained from the LIDAR observations. When compared to traditional ground-based Ceilometer retrieval techniques, includes depend on micro pulse LiDAR information under RL conditions.

Considering the approximation of BL elevations: a ML methodology was introduced by Krishnamurthy et al. [57]. One of the most important parameters in atmospheric models for computing the heat, momentum, and moisture exchange among the surface and the free troposphere is the planetary boundary layer height (z j). This study creates and evaluates aWavelet techniques utilized for LIDAR identification of PBLH under normal ML approach for z j estimation using a 4-yearconditions, the ML-PBLH detection algorithm shows encouraging early findings. Dense clouds restrict the application of both the wavelet method and conventional methods for LIDAR backscatter retrievals. However, the suggested machine learning method may dataset in the Southern Great Plains site from 2016 to 2019. An RF model is fed parameters gathered from Doppler lidars along with more than twenty various surface meteorological observations. The model is evaluated using data from 2019 after it was trainedidentify PBLH in these situations. utilizing radiosonde-derived z j values for theML-Based BLH Estimation through LiDAR Data in Complex Atmospheric Situations was suggested by, Liu et al. [56]. In this research, first ML approach to compute ABLH has difficult atmospheric conditions utilizing just LiDAR-depend equipment is proposed: the Mahalanobis transform K-near- means (MKnm) method. It was used on the micro pulse LiDAR data that was collected at the Atmospheric Radiation Measurement (ARM) program's Southern Great Plains site. Several methods were used to determine the diurnal cycles of ABLH from cloudy weather: gradient method, K-means, MKnm as well as wavelet covariance transform technique (WM). The reference height resulting through radiosonde information was compared with the ABLH determined on each of those methods years 2016 through 2018. 2019 results demonstrated a significantly greater agreement across the radiosonde when compared to estimates obtained from a thresholding method that only employed Doppler lidars.

Mei et al. [58] suggested a Planetary boundary layer height retrieval using lidar data and a deep learning technique based on the wavelet covariance transform. In this study, provide a unique deep-learning technique for the PBLH evaluation using atmospheric lidar assessments, depending on the wavelet covariance transform (WCT). To create 2-dimensional wavelet images, lidar profiles are analyzed using a range of dilation values between 200 m to 505 m in accordance with the WCT. A CNN is developed based on a modified VGG16- CNN, and a large number of wavelet images and the matching PBLH- labelled images are created as the training set. In addition, a test set of wavelet images derived from lidar profiles has been produced in order to examine the CNN's performance. By analyzing the wavelet coefficients and the expected PBLH-labelled image, the PBLH is ultimately retrieved.

Reuter et al. [59] suggested an Ensemble-based satellite-derived database (2003–2018) both climate as well as carbon applications that are column-general for methane along with carbon dioxide. Here, a new data sets that are the result of combining multiple separate satellite data produce consistent

long-term climate data records for 2 Essential Climate Variables (ECVs). The Orbiting Carbon Observatory 2 (OCO-2) satellite data was also used for the first time (for XCO2) in these ECV CDRs, which span the years 2003–2018. The data products gathered by the satellite sensors TANSO-FTS/GOSAT as well as SCIAMACHY/ ENVISAT have been combined to create the ensemble. The L2 products are made up of daily Network Common Data Form (NetCDF) records that consist of typical kernel through every solitary satellite observation, along with corresponding estimations of uncertainty for random as well potential systematic uncertainties, however the important parameters, such as XCH4 or XCO2.

Table 4: Comparison of machine learning in ABLH

Authors	Contribution	Advantages	Limitations
[48]	Using AERI measurement data, a new machine learning approach for planetary boundary layer height calculate	When it comes to temporal resolution, AERI data is superior to radiosondes.	Limited data accessibility
[49]	Prediction of Planetary Boundary Layer Height from Lidar Data using the Combination of Machine Learning Algorithms and the Gradient Method	Enhanced Accuracy	Training Machine learning model might require a lot of processing power.
[50]	Using machine learning approaches to estimate the height of the urban atmospheric boundary layer through remote sensing	Complex situations can be handled via machine learning.	Interpreting complex models can be challenging.
[51]	Application of the k-nearest neighbours' algorithm, IIR shelving filter, and support vector machine for short-duration RMS changes and voltage transients	Performs well even with a small quantity of training data.	Can be costly to compute for huge datasets.

Authors	Contribution	Advantages	Limitations
[52]	An evaluation of the possibilities and limits of ground-based remote sensing through measuring the height of the ABL	It can easily combine the data	Depending on the device and the weather, range can change.
[53]	Naive Bayes classifiers, probability, and impact echo data are used for bridge monitoring and fault identification.	Handles big datasets	Sensitive to minor Features
[54]	LSTM network-based prediction of the height of the temporal ABL	For predicting ABL height, LSTMs perform better.	Restricted interpret ability
[55]	A deep machine learning technology for boundary level detection using lidar	Improved Capability to Generalize	Deep learning methods suffer high computational costs.
[56]	ML for estimating BLH from lidar data in difficult atmospheres.	Enhanced Accuracy in Complicated Conditions	Explainability problems
[57]	About the approximation of BLH: a ML methodology	Computationally efficient	BLH could be difficult to understand.
[58]	PBLH retrieval using lidar data and a DL technique based upon the wavelet covariance transform	Computationally efficient	BLH could be difficult to understand.
[58]	PBLH retrieval using lidar data and a DL technique based upon the wavelet covariance transform	High accuracy	Time-consuming
[59]	Ensemble-based satellite-derived data sets (2003–2018) on carbon as well as weather cases that are column-averaged for carbon dioxide and methane	Extended data coverage	Restricted spatial resolution

2.7. Metrics and Graphs used for monitoring ABLH

In this review article, the metrics used for monitoring ABLH is RMSE, MSE, MAPE etc. A collection of ABLH temporal sequence serve through the input data for the problem of ABL height prediction. The unseen layer of the preceding opinion will influence the hidden film of the following opinion as the series carries along. Figure 9 shows the line graph of temporal average of the predicted and observed ABL height data.

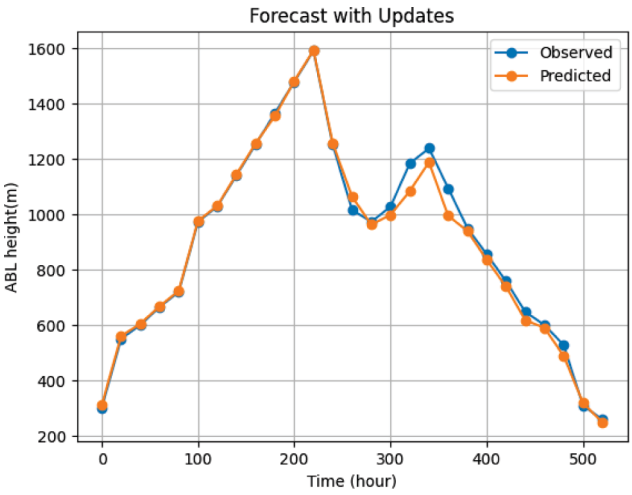

Figure 9: Comparison of observed and predicted ABLH data.

The height of the atmospheric boundary layer (ABL) is predicted using an ABL height forecast. The lowest region of the atmosphere which is affected by the surface of the Earth is the ABL. Here, by varying time, the ABL height is calculated. Considering thegreatest value of ABL height through SODAR 1775 m, predicted in the machine learning. signifies the updated net through predicted cost (1650 m maximum). Figure 10 indicates the comparison of Time vs error rate.

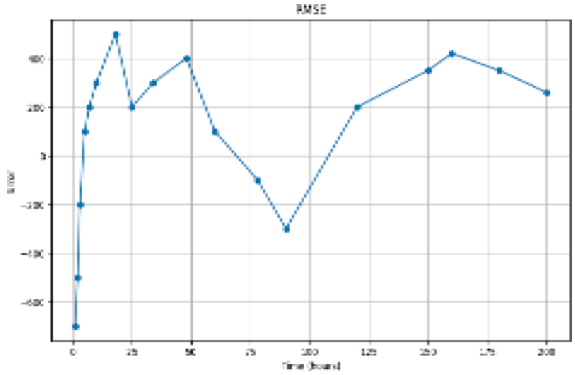

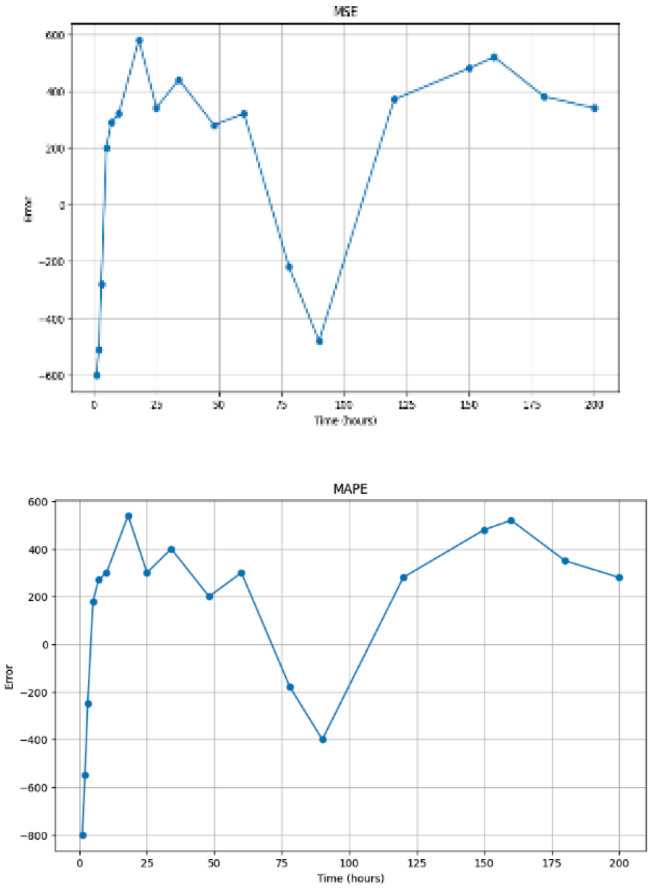

Figure 10: Comparison of Time vs error rate

Root Mean Squared Error is referred toas RMSE. It is a commonly utilized metric that calculates the difference between expected and actual values to evaluate how accurate a prediction is. In simple terms, it indicates the degree to which the predictions and the actual events matched. A model or forecasting technique is considered as having better if the RMSE was lower. Here, by varying time the error rate is calculated. A measure of forecast or prediction accuracy compared to actual values is the Mean Absolute Percentage Error, or MAPE. Because the error is presented as a percentage, it is easier to understand and explain the accuracy on the model. Figure 11 indicates the comparison of month variations in ABLH.

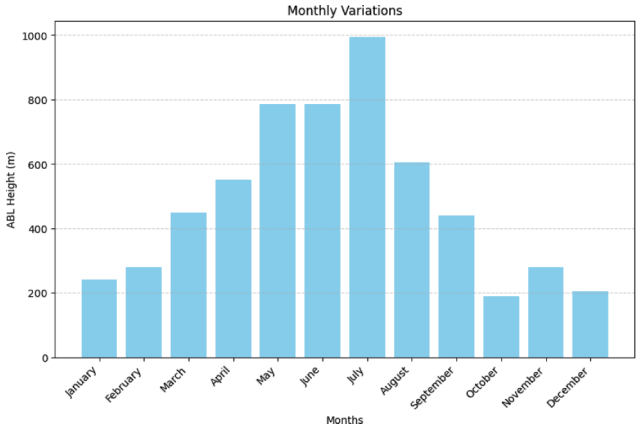

a)

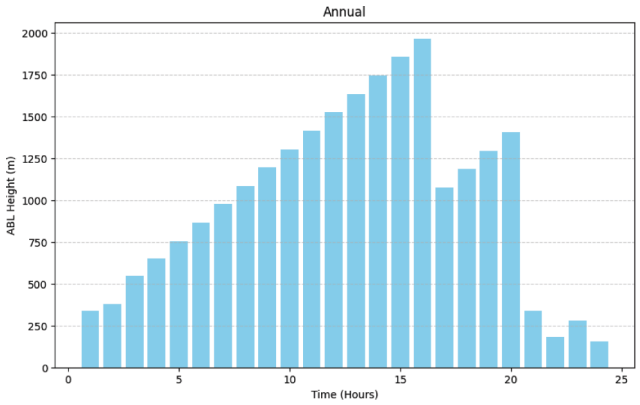

b)

Figure 11 (a)-(b): Monthly as well as Temporal Variations inside Annual ABL Height.

Throughout the year, there are both temporal (daily) and monthly changes in the height of the Atmospheric Boundary Layer (ABL). Because of the intense solar heating that occurs in the afternoon, between 11 AM and 2 PM, the ABL height is typically at its maximum. The warmest months are usually when ABL height is at its highest point. This is because an environment that is warmer experiences increased convection. However, weaker solar heating and decreased convection cause the ABL height to be lowest during the coldest months (such as winter).

III. CONCLUSION

This review paper discusses the most effective ways to utilize ground-based machine learning techniques to obtain a thorough understanding of the heights and dynamics of the ABL sub-layer. Firstly, the explanation about sublayers of ABLH is considered. The sublayers of ABLH are surface layer, Daytime entrainment zone or nighttime capping inversion and residual layer. The Earth's surface immediately affects the surface layer, which is regular and swift variations in wind speed, humidity, and temperature. A residue layer develops as a result of the PBL's daytime mixing. The atmospheric boundary layer (ABL), the lowest layer of the atmosphere that is directly affected by the Earth's surface, contains the layers known as the daytime entrainment zone and the nighttime capping inversion. Next is characterization of atmospheric gas and thermodynamics variables include: temperature, humidity, nitrogen, oxygen etc. Next is the classification of ABLH, these techniques usually utilize wind speed, humidity, and temperature data gathered from the atmosphere. The top of the ABL, or the separation between the turbulent ABL as well as the more stable free troposphere above, can be found by scientists by examining these measurements. Next is some of the machine learning techniques used for ABLH monitoring. In general, machine learning offers promising paths toward accurate and successful ABLH monitoring. The available sensors, accessible processing power, and required forecast speed influence the approach selection. Researchers conclude that large-resolution measurements through the ABL, which remains the greatest under tested region of the air, can be obtained through ground-based ABLH.

REFERENCES

[1] Kulmala, Markku, Tom Kokkonen, Ekaterina Ezhova, Alexander Baklanov, Alexander Mahura, Ivan Mammarella, Jaana Bäck et al. "Aerosols, clusters, greenhouse gases, trace gases and boundary-layer dynamics: on feedbacks and interactions." Boundary-Layer Meteorology 186, no. 3 (2023): 475-503.

[2] Vieira dos Santos, Amanda, Elaine Cristina Araújo, Izabel da Silva Andrade, Thais Corrêa, Márcia Talita Amorim Marques, Carlos Eduardo Souto-Oliveira, Noele Franchi Leonardo et al. "Comparison of PBL Heights from Ceilometer Measurements and

Greenhouse Gases Concentrations in São Paulo." Atmosphere 14, no. 12 (2023): 1830.

[3] Kumar, C. Navin, N. Thavaprakaash, S. Panneerselvam, and S. Arul Prasad. "Atmospheric Boundary Layer and Geographic Information System (GIS): A Review." GIScience for the Sustainable Management of Water Resources (2022): 385-400.

[4] Jaiswal, Krishna Kumar, Chandrama Roy Chowdhury, Deepti Yadav, Ravikant Verma, Swapnamoy Dutta, Km Smriti Jaiswal, and Karthik Selva Kumar Karuppasamy. "Renewable and sustainable clean energy development and impact on social, economic, and environmental health." Energy Nexus 7 (2022): 100118.

[5] Kumar, Nishant, Kirti Soni, and Ravinder Agarwal. "Variation of Atmospheric Boundary Layer Height and Application of ForwardSelection Technique during Diwali." In International Conference On" Advances In Metrology", pp. 113-125. Singapore: Springer Nature Singapore, 2022.

[6] Harm-Altstädter, Barbara. "Atmospheric boundary layer dynamics and aerosol properties based on observations of unmanned research aircraft." PhD diss., Dissertation, Braunschweig, Technische Universität Braunschweig, 2021, 2022.

[7] Li, Hui, Zhangjun Wang, Quanfeng Zhuang, Rui Wang, Wentao Huang, Chao Chen, Xianxin Li et al. "Remote Polar Boundary Layer Wind Profiling Using an All-Fiber Pulsed Coherent Doppler Lidar at Zhongshan Station, Antarctica." Atmosphere 14, no. 5 (2023): 901.

[8] Wu, Dong L., Jie Gong, and Manisha Ganeshan. "GNSS-RO Deep Refraction Signals from Moist Marine Atmospheric Boundary Layer (MABL)." Atmosphere 13, no. 6 (2022): 953.

[9] Summa, Donato, Fabio Madonna, Noemi Franco, Benedetto De Rosa, and Paolo Di Girolamo. "Inter-comparison of atmospheric boundary layer (ABL) height estimates from different profiling sensors and models in the framework of HyMeX-SOP1." Atmospheric Measurement Techniques 15, no. 14 (2022):4153-4170.

[10] Molero, Francisco, Rubén Barragán, and Begoña Artíñano. "Estimation of the atmospheric boundary layer height by means of machine learning techniques using ground- level meteorological data." Atmospheric Research 279 (2022): 106401.

[11] Ortiz-Amezcua, Pablo, Juana Andújar- Maqueda, Antti J. Manninen, Pyry Pentikäinen, Ewan J. O'Connor, Iwona S. Stachlewska, Gregori de Arruda Moreira et al. "Dynamics of the Atmospheric Boundary Layer over two middle-latitude rural sites with Doppler lidar." Atmospheric Research 280 (2022):106434.

[12] Qiu, Cong, Xiaoming Wang, Haobo Li, Kai Zhou, Jinglei Zhang, Zhe Li, Dingyi Liu, and Hong Yuan. "A Comparison of Atmospheric Boundary Layer Height Determination Methods Using GNSS Radio Occultation Data." Atmosphere 14, no. 11 (2023): 1654.

[13] Giani, Paolo, and Paola Crippa. "On the Sensitivity of Large Eddy Simulations of the Atmospheric Boundary Layer Coupled with Realistic Large Scale Dynamics." Monthly Weather Review (2024).

[14] Burgos-Cuevas, Andrea, Adolfo Magaldi, David K. Adams, Michel Grutter, Jorge L. García Franco, and Angel Ruiz-Angulo. "Boundary layer height characteristics in Mexico City from two remote sensing techniques." Boundary-Layer Meteorology 186, no. 2 (2023): 287-304.

[15] Summa, Donato, Gemine Vivone, Noemi Franco, Giuseppe D'Amico, Benedetto De Rosa, and Paolo Di Girolamo. "Atmospheric Boundary Layer Height: Inter-Comparison of Different Estimation Approaches Using the Raman Lidar as Benchmark." Remote Sensing 15, no. 5 (2023): 1381.

[16] Anand, Michael, and Sandip Pal. "Exploring atmospheric boundary layer depth variability in frontal environments over an arid region." Boundary-Layer Meteorology 186, no. 2 (2023): 251-285.

[17] Bellini, Annachiara, Henri Diémoz, Luca Di Liberto, Gian Paolo Gobbi, Alessandro Bracci, Ferdinando Pasqualini, and Francesca Barnaba. "Alicenet–An Italian network of Automated Lidar-Ceilometers for 4D aerosol monitoring: infrastructure, data processing, and applications." EGUsphere 2024 (2024): 1-47.

[18] Inoue, Jun, and Kazutoshi Sato. "Toward sustainable meteorological profiling in polar regions: Case studies using an inexpensive UAS on measuring lower boundary layers with quality of radiosondes." Environmental Research 205 (2022): 112468.

[19] Zhang, Damao, Jennifer Comstock, and Victor Morris. "Comparison of planetary boundary layer height from ceilometer with ARM radiosonde data." Atmospheric Measurement Techniques 15, no. 16 (2022): 4735-4749.

[20] Chen, Yehui, Xiaomei Jin, Ningquan Weng, Wenyue Zhu, Qing Liu, and Jie Chen. "Simultaneous extraction of planetary boundary-layer height and aerosol optical properties from coherent doppler wind lidar." Sensors 22, no. 9 (2022): 3412.

[21] Guan, Yi, JinRong Wang, and Michal Feckan. "Explicit solution and dynamical properties of atmospheric Ekman flows with boundary conditions." Electronic Journal of Qualitative Theory of Differential Equations 2021, no. 30 (2021): 1-19.

[22] Khalesi, Bahareh, and Mohammad Reza Mansouri Daneshvar. "Comprehensive temporal analysis of temperature inversions across urban atmospheric boundary layer of Tehran within 2014–2018." Modeling Earth Systems and Environment 6, no. 2 (2020): 967-982.

[23] Wang, Yonghong, Yongjing Ma, Chao Yan, Lei Yao, Runlong Cai, Shuying Li, Zhuohui Lin et al. "Sulfur dioxide transported from the residual layer drives atmospheric nucleation during haze periods in Beijing." Geophysical Research Letters 50, no. 6 (2023): e2022GL100514.

[24] Sherbo, Rebecca S., Pamela A. Silver, and Daniel G. Nocera. "Riboflavin synthesis from gaseous nitrogen and carbon dioxide by a hybrid inorganic-biological system." Proceedings of the National Academy of Sciences 119, no. 37 (2022): e2210538119.

[25] Lee, Hyeonseok, John R. Klaehn, Christopher J. Orme, Joshua S. McNally, Aaron D. Wilson, Frederick F. Stewart, and Birendra Adhikari. "Molecular dynamics study of carbon dioxide and nitrogen selectivity through poly [bis ((methoxyethoxy) ethoxy) phosphazene](MEEP) membrane." Chemical Engineering Science 284 (2024): 119480.

[26] Wen, Zhang, Wen Xu, Qi Li, Mengjuan Han, Aohan Tang, Ying Zhang, Xiaosheng Luo et al. "Changes of nitrogen deposition in China from 1980 to 2018." Environment International 144 (2020): 106022.

[27] Morelli, Alessandro Maria, and Felix Scholkmann. "The Significance of Lipids for the Absorption and Release of Oxygen in Biological Organisms." In International Society on Oxygen Transport to Tissue, pp. 93- 99. Cham: Springer International Publishing, 2022.

[28] Graven, Heather, Ralph F. Keeling, and Joeri Rogelj. "Changes to carbon isotopes inatmospheric CO2 over the industrial era and into the future." Global Biogeochemical Cycles 34, no. 11 (2020): e2019GB006170.

[29] Xie, Cong, Xin Zhang, Long Zhuang, Ruixi Zhu, and Jie Guo. "Analysis of surface temperature variation of lakes in China using MODIS land surface temperature data." Scientific Reports 12, no. 1 (2022): 2415.

[30] Phillips, Helen E., Amit Tandon, Ryo Furue, Raleigh Hood, Caroline Ummenhofer, Jessica Benthuysen, Viviane Menezes et al. "Progress in understanding of Indian Ocean circulation, variability, air-sea exchange and impacts on biogeochemistry." Ocean Science Discussions 2021 (2021): 1-109.

[31] Marley, Hannah Gwen. "A Quantitative Analysis of the Atmospheric Boundary Layer and Air Pollution Factors Determining the Formation of Winter Brown Haze in an Urban Area of Complex Coastal Terrain." PhD diss., ResearchSpace@ Auckland, 2023.

[32] Giovannini, Lorenzo, Enrico Ferrero, Thomas Karl, Mathias W. Rotach, Chantal Staquet, Silvia Trini Castelli, and Dino Zardi. "Atmospheric pollutant dispersion over complex terrain: Challenges and needs for improving air quality measurements and modeling." Atmosphere 11, no. 6 (2020): 646.

[33] Che, Junhui, and Ping Zhao. "Characteristics of the summer atmospheric boundary layer height over the Tibetan Plateau and influential factors." Atmospheric Chemistry and Physics 21, no. 7 (2021): 5253-5268.

[34] Lelandais, Ludovic, Irène Xueref-Remy, Aurelie Riandet, Pierre-Eric Blanc, Alexandre Armengaud, Sonia Oppo, Christophe Yohia, Michel Ramonet, and Marc Delmotte. "Analysis of 5.5 years of atmospheric CO2, CH4, CO continuous observations (2014–2020) and their correlations, at the Observatoire de Haute Provence, a station of the ICOS-France national greenhouse gases observation network." Atmospheric Environment 277 (2022): 119020.

[35] Sommerfeld, Markus. "Optimal performance of airborne wind energy systems subject to realistic wind profiles." PhD diss., 2020.

[36] Han, Bisen, Tian Zhou, Xiaowen Zhou, Shuya Fang, Jianping Huang, Qing He, Zhongwei Huang, and Minzhong Wang. "A New Algorithm of Atmospheric Boundary Layer Height Determined from Polarization Lidar." Remote Sensing 14, no. 21 (2022): 5436.

[37] Wu, Changcai, Yajie Ma, Dan Wang, Yongpan Shan, Xianpeng Song, Hongyan Hu, Xiangliang Ren, Xiaoyan Ma, Jinjie Cui, and Yan Ma. "Integrated microbiology and metabolomics analysis reveal plastic mulch film residue affects soil microorganisms and their metabolic functions." Journal of Hazardous Materials 423 (2022): 127258.

[38] Bedoya-Velásquez, Andres Esteban, Romain Ceolato, Gloria Titos, Juan Antonio Bravo-Aranda, Andrea Casans, Diego Patrón, Sol Fernández-Carvelo, Juan Luis Guerrero- Rascado, and Lucas Alados-Arboledas. "Synergy between Short-Range Lidar and In Situ Instruments for Determining the Atmospheric Boundary Layer Lidar Ratio." Remote Sensing 16, no. 9 (2024): 1583.

[39] Zhang, Yuanjie, Kang Sun, Zhiqiu Gao, Zaitao Pan, Michael A. Shook, and Dan Li. "Diurnal climatology of planetary boundary layer height over the contiguous United States derived from AMDAR and reanalysis data." Journal of Geophysical Research: Atmospheres 125, no. 20 (2020): e2020JD032803.

[40] Garnés-Morales, Ginés, Maria João Costa, Juan Antonio Bravo-Aranda, María José Granados-Muñoz, Vanda Salgueiro, Jesús Abril-Gago, Sol Fernández-Carvelo et al. "Four Years of Atmospheric Boundary Layer Height Retrievals Using COSMIC-2 Satellite Data." Remote Sensing 16, no. 9 (2024): 1632.

[41] Wu, Yonghua, Kaihui Zhao, Xinrong Ren, Russell R. Dickerson, Jianping Huang, Margaret J. Schwab, Phillip R. Stratton, Hannah Daley, Dingdong Li, and Fred Moshary. "Ozone pollution episodes and PBL height variation in the NYC urban and coastal areas during LISTOS 2019." Atmospheric Environment 320 (2024): 120317.

[42] Layer, A. B. (2023, December). Observation of Structure of Marine Atmospheric Boundary Layer by Ceilometer Over the Kuroshio Current Toshiyuki Murayama and Fumiaki Kobashi. In Proceedings of the 30th International Laser Radar Conference (p. 453). Springer Nature.

[43] Liu, Cheng, Jianping Huang, Yongwei Wang, Xinyu Tao, Cheng Hu, Lichen Deng, Jiaping Xu et al. "Vertical distribution of PM2. 5 and interactions with the atmospheric boundary layer during the development stage of a heavy haze pollution event." Science of the Total Environment 704 (2020): 135329.

[44] Osibanjo, O. O., B. Rappenglück, and A. Retama. "Anatomy of the March 2016 severe ozone smog episode in Mexico- City." Atmospheric Environment 244 (2021):117945.

[45] Mei, Shuo-Jun, and Chao Yuan. "Urban buoyancy-driven air flow and modelling method: A critical review." Building and Environment 210 (2022): 108708.

[46] Kakkanattu, Sachin Philip, Sanjay Kumar Mehta, D. Bala Subrahamanyam, V. Rakesh, and Amit P. Kesarkar. "Thermodynamic structure of the atmospheric boundary layer over a coastal station in India for contrasting sky conditions during different seasons." Atmospheric Research 293 (2023):106915.

[47] Cannaby, Heather, and Martin White. "The impact of topography and rotation in shaping the basin-scale circulation in Lough Corrib, Ireland, under homogenous conditions." Irish Journal of Earth Sciences (2023).

[48] Ye, Jin, Lei Liu, Qi Wang, Shuai Hu, and Shulei Li. "A novel machine learning algorithm for planetary boundary layer height estimation using AERI measurement data." IEEE Geoscience and Remote Sensing Letters 19 (2021): 1-5.

[49] Li, Hui, Boming Liu, Xin Ma, Shikuan Jin, Weiyan Wang, Ruonan Fan, Yingying Ma, Ruyi Wei, and Wei Gong. "Estimation of Planetary Boundary Layer Height From Lidar by Combining Gradient Method and Machine Learning Algorithms." IEEE Transactions on Geoscience and Remote Sensing (2023).

[50] de Arruda Moreira, Gregori, Guadalupe Sánchez-Hernández, Juan Luis Guerrero-Rascado, Alberto Cazorla, and Lucas Alados- Arboledas. "Estimating the urban atmospheric boundary layer height from remote sensing applying machine learning techniques." Atmospheric Research 266 (2022): 105962.

[51] Liubčuk, Vladislav, Gediminas Kairaitis, Virginijus Radziukynas, and Darius Naujokaitis. "IIR shelving filter, support vector machine and k-nearest neighbors algorithm application for voltage transients and short- duration RMS variations analysis." Inventions 9, no. 1 (2024): 12.

[52] Kotthaus, Simone, Juan Antonio Bravo- Aranda, Martine Collaud Coen, Juan Luis Guerrero-Rascado, Maria João Costa, Domenico Cimini, Ewan J. O'Connor et al. "Atmospheric boundary layer height from ground-based remote sensing: a review of capabilities and limitations." Atmospheric Measurement Techniques 16, no. 2 (2023): 433-479.

[53] Jafari, Faezeh, and Sattar Dorafshan. "Bridge inspection and defect recognition with using impact echo data, probability, and Naive Bayes classifiers." Infrastructures 6, no. 9 (2021): 132.

[54] Kumar, Nishant, Kirti Soni, and Ravinder Agarwal. "Prediction of temporal atmospheric boundary layer height using long short-term memory network." Tellus A: Dynamic Meteorology and Oceanography 73, no. 1 (2021): 1-14.

[55] Sleeman, Jennifer, Milton Halem, Zhifeng Yang, Vanessa Caicedo, Belay Demoz, and Ruben Delgado. "A deep machine learning approach for lidar based boundary layer height detection." In IGARSS 2020-2020 IEEE international geoscience and remote sensing symposium, pp. 3676-3679. IEEE, 2020.

[56] Liu, Zhenxing, Jianhua Chang, Hongxu Li, Sicheng Chen, and Tengfei Dai. "Estimating boundary layer height from lidar data under complex atmospheric conditions using machine learning." Remote Sensing 14, no. 2 (2022): 418.

[57] Krishnamurthy, Raghavendra, Rob K. Newsom, Larry K. Berg, Heng Xiao, Po-Lun Ma, and David D. Turner. "On the estimation of boundary layer heights: a machine learning approach." Atmospheric Measurement Techniques 14, no. 6 (2021): 4403-4424.

[58] Mei, Liang, Xiaoqi Wang, Zhenfeng Gong, Kun Liu, Dengxin Hua, and Xiaona Wang. "Retrieval of the planetary boundary layer height from lidar measurements by a deep- learning method based on the wavelet covariance transform." Optics Express 30, no. 10 (2022): 16297-16312.

[59] Reuter, Maximilian, Michael Buchwitz, Oliver Schneising, Stefan Noël, Heinrich Bovensmann, John P. Burrows, Hartmut Boesch et al. "Ensemble-based satellite-derived carbon dioxide and methane column-averaged dry-air mole fraction data sets (2003–2018) for carbon and climate applications." Atmospheric Measurement Techniques 13, no. 2 (2020): 789